Modelling and Simulation of Acoustic Absorption of Open Cell Metal Foams

Claudia Lautensack, Matthias Kabel
Fraunhofer ITWM, Kaiserslautern

Abstract

We analyse the microstructure of an open nickel-chrome foam using computed tomography. The foam sample is modelled by a random Laguerre tessellation, i.e. a weighted Voronoi tessellation, which is fitted to the original structure by means of geometric characteristics estimated from the CT image. Using the Allard-Johnson model we simulate the acoustic absorption of the real foam and the model. Finally, simulations in models with a larger variation of the cell sizes yield first results for the dependence of acoustic properties on the geometric structure of open cell foams.

1. Introduction

Open cell metal foams are versatile materials which are used in many application areas, e.g. as heat exchangers, catalysts or sound absorbers. The physical properties of a foam are highly affected by its microstructure, for instance the porosity or the specific surface area of the material or the size and shape of the foam cells. An understanding of the change of the foam's properties with altering microstructure is crucial for the optimisation of foams for certain applications. Foam models from stochastic geometry are powerful tools for the investigation of these relations.
Edge systems of random tessellations are often used as models for open foams. Geometric characteristics which are estimated from tomographic images of the foams are used for fitting the models to real data. Realisations of foams with slightly modified microstructure can then be generated by changing the model parameters. Numerical simulations in these virtual foam samples allow for an investigation of relations between the geometric structure of a material and its physical properties.
In the field of low noise applications open cell metal foams are used e.g. for blow down silencers and control valves. Since the acoustic properties depend on the flow resistance of the metal foam inserts, an understanding of the dependency of the flow resistance on the geometry of the metal foam is necessary for the optimisation of the inserts.
In this paper, the cell structure of an open metal foam is analysed using a tomographic image of the material. Based on the estimated characteristics a Laguerre tessellation model is fitted to the foam structure. Acoustic absorption is calculated in both the original and the model structure. The variation of structure parameters then allows to study relations between the microstructure of the material, e.g. the cell size variation, and its acoustic properties.

2. Analysis of the CT data

The material under consideration is a nickel-chrome foam provided by Recemat International (RCM-NC-2733.10). Our investigation is based on a tomographic grey value image of the

material with a voxel edge length of 3.14 μm and 800 × 1600 × 1600 voxels which corresponds to a 2.512 × 5.024 × 5.024 mm³ sample. A visualisation is shown in Figure 1.

FIGURE 1: Visualisation of a subsample of the metal foam.

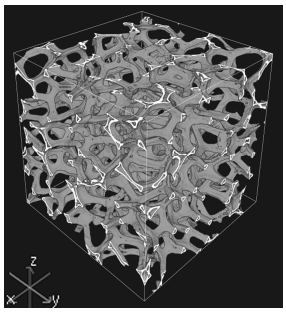

In order to relate the acoustic properties of the foam to certain geometric features and to fit a model to the data we are aiming at a description of the geometry of the foam cells by means of characteristics such as their volume, diameter or shape. To measure these characteristics from the CT image of the foam sample, the foam cells are reconstructed, i.e. the pore space of the material is separated into single cells.
First, the volume image is binarised using a local thresholding approach (Niblack thresholding, (11)). To avoid reconstruction errors caused by the hollow edges of the foam, the edges are filled by a morphological closing. To the resulting binary image, the cell reconstruction method described in (13) is applied. Sections of the resulting images are shown in Figure 2. For all image processing steps we use the MAVI software package (6).

FIGURE 2: Sections of the original image, the binarisation, the image with closed edges, and the reconstructed cells (from left to right).

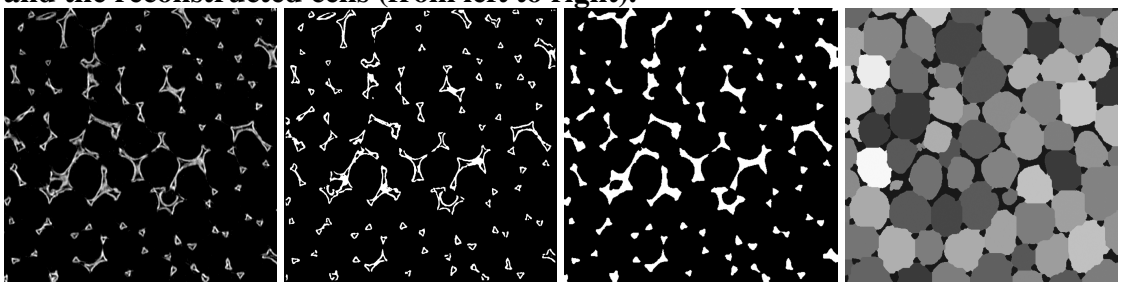

The geometric characteristics of the reconstructed foam cells are estimated from the image using the ObjectFeatures function of MAVI. A minus-sampling edge correction is used to avoid edge effects caused by cells intersecting the image boundary. It turned out that the mean cell diameter in z-direction differs from the means in x- and y-direction by a factor of 0.856. An isotropic structure is obtained by an appropriate scaling of the z-axis. The mean values and standard deviations of the volume, surface area, diameter, and number of facets of the scaled foam cells are shown in Table 1.

3. Modelling

The foam is modelled by the edge system of a random Laguerre tessellation. This generalisation of the well-known Voronoi tessellations is defined as follows.
Denote by s(x,r) a sphere in R^d with center $x \in R^d$ and radius $r \geq 0$ and let S be a locally finite set of spheres, which means that each bounded subset of R^d is

intersected only by a finite number of spheres. The Laguerre cell C(s(x,r),S) generated by a sphere s(x,r) consists of all points $y \in R^d$ which are closest to s(x,r) with respect to the so-called power distance $pow(y, s(x,r)) = \|x-y\|^2-r^2$, where $\|\cdot\|$ denotes the Euclidean distance. That means

$$C(s(x,r), S) = \{y \in R^d : pow(y, s(x,r)) \leq pow(y, s(x',r')) \text{ for all } s(x',r') \in S\}. \quad (1)$$

The Laguerre tessellation L(S) is the set of Laguerre cells of spheres contained in S. It is a space-filling system of convex polytopes. If the spheres in S do not overlap, each cell completely contains its generating sphere. If all radii are equal, L(S) equals the Voronoi tessellation of the set of sphere centres.
For the set of generators we choose a random sphere packing simulated using the force biased algorithm (1) which results in tessellations with very regular cell shapes but variable size distribution. Geometric characteristics of the cells in a Laguerre tessellation generated by sphere packings with lognormal or gamma distributed volumes are reported in (12). Using these results we may fit a Laguerre tessellation model to the real data without further simulation. The parameters of the model are the packing density φ and the coefficient of variation (CV) of the volume distribution of the generating sphere packing. The deviation of the models from the foam sample is measured using the relative distance measure

$$D(m,c) = \sqrt{\sum_{i=1}^{8} \left(\frac{m_i - c_i}{c_i} \right)^2}, \quad (2)$$

where the eight entries of $c=(c_1,\ldots, c_8)$ and $m=(m_1,\ldots, m_8)$ are the means and standard deviations of the volume v, surface area s, number of facets f, and diameter d of the cells of the original foam and the model, respectively.
Using this procedure, a Laguerre tessellation generated by a sphere packing with lognormal volume distribution with the parameters $\varphi = 0.6$ and CV = 0.3328 is found to be the best-fit model. The geometric characteristics of the model structure are shown in Table 1.

TABLE 1. Estimated Mean Values and Standard Deviations of Cell Characteristics of the Foam sample and the fitted Laguerre Tessellation.

	scaled data		model			
	mean	sd	mean	deviation[%]	sd	deviation[%]
v [mm³]	0.1283	0.0342	0.1283	0.00	0.0347	+ 1.35
s [mm²]	1.4218	0.2434	1.3588	- 4.43	0.2281	- 6.28
d [mm]	0.6890	0.0568	0.6822	- 0.99	0.0579	+ 1.93
f	13.810	1.705	14.103	+ 2.12	1.922	+12.76

The tessellations are scaled in z-direction by a factor of 0.856 and their edges are dilated such that the volume fraction fits the value of 0.1023 observed in the real data. As structuring element of the dilation we use a ball of constant size (classical dilation). Furthermore, a second sample is generated where the size of the ball varies with respect to distance to the vertices as observed in the real data (locally adaptable dilation, see (10)). Due to the dilation with a ball, the edges in the model structures show circular cross sections, in contrast to the triangular edges in the real foam. In order to study the influence of the cross section shape, we

also generate a version of the real foam with circular edge cross sections via dilation of the skeleton of the edge system. Visualisations of all structures are shown in Figure 3.

FIGURE 3: Visualisations of the original foam with closed edges, the original foam with circular edges, the classical and the adaptable dilation of the Laguerre model and the PV model.

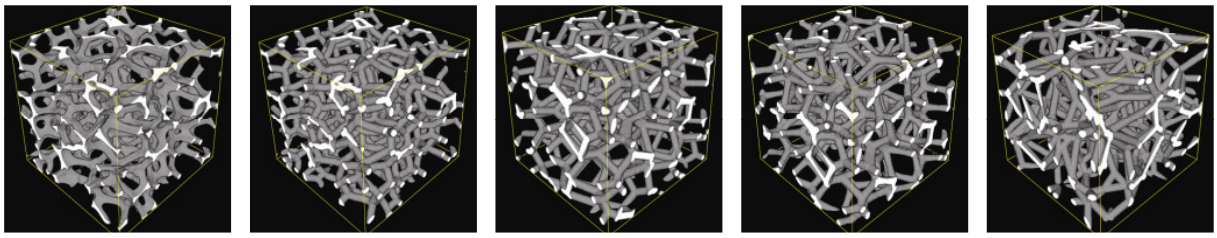

data | data circular | Lag, CV=0.33 | Lag adaptable | PV

4. Simulation of acoustic absorption

In contrast to the more sophisticated model of Biot (2), the model of Allard-Johnson (1) describes the macroscopic propagation of sound in porous media with rigid frames based only on geometric parameters. It is used to replace the porous material by an equivalent fluid. The acoustic properties of a fluid are described by the wave number $k = \omega\sqrt{\rho_0 / K_f}$ and the characteristic impedance $Z_c = \sqrt{\rho_0 K_f}$, where K_f and ρ_0 are the bulk modulus and the density of the fluid, respectively.

To describe dissipative processes in the macroscopic description of sound propagation, that is the wave equation, the bulk modulus and the density are replaced by complex quantities depending on the pore space.

With Φ, σ, α_∞, Λ, and Λ' denoting the open porosity, the flow resistance, the tortuosity, the viscous length, and the thermal length, Allard and Johnson derived the following equations for the effective bulk modulus K and the effective density ρ in the case of porous materials with cylindrical pores

$$K = \gamma P_0 \left[\gamma - (\gamma - 1) \left[1 + \frac{8\eta_0}{i\omega\rho_0 \Lambda'^2 B} \sqrt{1 + \frac{i\omega\rho_0 \Lambda'^2 B}{16\eta_0}} \right]^{-1} \right]^{-1}, \text{ and}$$

$$\rho = \rho_0 \alpha_\infty \left[1 + \frac{\sigma\Phi}{i\omega\rho_0\alpha_\infty} \sqrt{1 + \frac{i4\omega\alpha_\infty^2 \eta_0 \rho_0}{\sigma^2 \Lambda^2 \Phi^2}} \right],$$

where ρ_0, η_0, γ, and B are the density, the dynamic viscosity, the adiabatic exponent, and the Prandtl number of the fluid (7,8).

The purely geometric parameters Φ, σ, α_∞, Λ, and Λ' are calculated from binary image data using the module AcoustoDict of GeoDict (4). By means of analytical solutions for the wave equation depending only on the effective bulk modulus, the effective density and the saturating fluid, the acoustic absorption coefficient for a layer of the material at normal incidence of the acoustic waves is calculated by the software tool AdOpt (5).

5. Results

The parameters for the Allard-Johnson model are determined for the real material and the model foams using AcoustoDict. Since in the Allard-Johnson model the frame is assumed to be rigid, we use the foam sample with closed edges for the determination of the parameters. To keep the computational effort limited, the calculation is restricted to images with a size of 400^3 voxels. Since the resolution of the foam image is suitably high, the image is downscaled by a factor of 2 such that the simulation covers a reasonable number of foam cells. The realisations of the model foams are generated at the same resolution.
The results of the simulations are shown in Table 2, where the values given for the model structures are the means of eight realisations. For comparison we also calculated the parameters of two Laguerre tessellations (Lag) generated by ball packings with a higher variation of cell sizes (CV = 0.66 and CV = 1.0) and of a Poisson Voronoi (PV) tessellation with the same number of cells as in the real sample.

TABLE 2. Simulated Parameters for the Computation of acoustic Absorption. The Flow is simulated along the z-Axis.

Sample	Φ [%]	σ [kg/m³s]	α_∞	Λ' [µm]	Λ [µm]
data	89.83	6377.21	1.15	343.71	308.69
data circular	89.55	5838.37	1.10	354.45	311.44
Lag, CV=0.33	89.85	5484.40	1.10	378.77	316.63
Lag, CV=0.66	89.73	5354.40	1.11	376.06	325.38
Lag, CV=1.0	89.86	5048.70	1.11	386.66	336.89
Lag adaptable	89.79	5322.23	1.10	386.88	330.39
PV	89.65	5023.40	1.11	374.37	313.33

In order to investigate the effect of the structure's anisotropy, the flow simulation was also carried out along the x-axis. In all cases the flow resistance turned out to be smaller than the values obtained for the z-direction. For the original structure, the value dropped by 10 %, while for all other structures reductions between 5 and 7 % were observed.
The absorption curves obtained from these simulations using the Allard-Johnson model are shown in Figure 4 (absorption coefficient at normal incidence for a 10 mm thick layer saturated with air at 20°C and 1013 mbar).

FIGURE 4: Acoustic absorption computed using the Allard-Johnson model. Simulation along the z-axis (left) and along the x-axis (right).

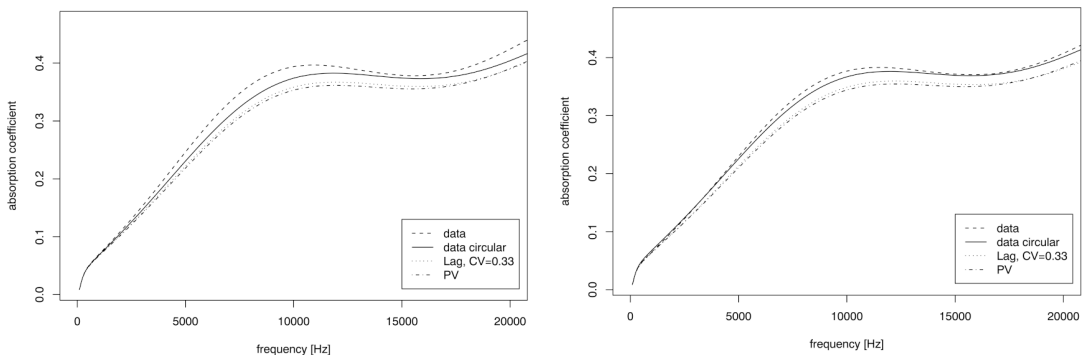

6. Discussion

The simulation results for the flow resistance show a large difference between the original foam sample with triangular edge cross section and its variation with circular cross section

shape. The same trend is observed in the absorption curves in Figure 4. Besides by the different cross section shape, this deviation can also be explained by the presence of closed facets in the original foam which are removed in its counterpart with circular edges. Consequently, the development of methods for the characterisation and modelling of various cross section shapes and closed facets could lead to more realistic models for the calculation of acoustic properties of open cell foams. Furthermore, the structural differences leading to the deviation between the modified data and the models have to be investigated.

Among the model structures, the classical dilation of the best-fit cell structure yields the best results. In particular, it performs better than the popular Poisson Voronoi tessellation. The adaptable dilation of the cell edges does not lead to better simulation results. However, in the foam sample studied in this paper, the variation of the thickness along the edges is only weakly pronounced. For foams with a stronger variation, the situation might be different.

A comparison of the three Laguerre tessellation models shows that a higher variation of the cell sizes in the foam leads to a reduction of the flow resistance. This suggests that homogeneous foams should be preferred as sound absorbers.

All structures under consideration show the same anisotropic behaviour. The acoustic absorption along the x-axis is slightly lower than along the z-axis which is due to the larger cell diameter in x-direction.

Altogether, our results indicate that Laguerre tessellations are suitable models for the investigation of acoustic properties of open cell foams. A more detailed analysis of the dependence of acoustic absorption on geometric characteristics such as cell size or shape could lead to a deeper understanding of how to choose foam materials for sound absorbers.

References

(1) J. F. Allard, Propagation of Sound in Porous Media: Modelling Sound Absorbing Materials. Elsevier, 1993

(2) M. A. Biot, Theory of Propagation of Elastic Waves in a Fluid-Saturated Porous Solid. I. Low-Frequency Range. II Higher Frequency Range, J. Acoust. Soc. Am. 1956, **28**, 168

(3) A. Bezrukov, M. Bargiel, D. Stoyan, Statistical analysis of simulated random packings of spheres, Part. Part. Syst. Charact. 2001, **19**, 111

(4) Fraunhofer ITWM, GeoDict, www.geodict.com

(5) Fraunhofer ITWM, AdOpt

(6) Fraunhofer ITWM, MAVI-Modular Algorithms for Volume Images, www.mavi-3d.de

(7) D. L. Johnson, J. Koplik, R. Dashen, Theory of dynamic permeability and tortuosity in fluid-saturated porous media, J. Fluid Mech. 1987, **176**, 379

(8) D. L. Johnson, J. Koplik, L. M. Schwartz, New pore-size parameter characterizing transport in porous media, Phys. Rev. Lett. 1986, **20**, 2564

(9) C. Lautensack, Fitting three-dimensional Laguerre tessellations to foam structures, J. Appl. Stat. 2008, **35** (9), 985

(10) C. Lautensack, M. Gietzsch, M. Godehardt, K. Schladitz, Modelling a ceramic foam using locally adaptable morphology, J. Microsc. 2008, **230** (3), 396

(11) W. Niblack, An introduction to Digital Image Processing, Prentice Hall, 1986

(12) C. Redenbach, Microstructure Models for Cellular Materials, accepted for publication in Computational Materials Science

(13) K. Schladitz, C. Redenbach, T. Sych, M. Godehardt, Microstructural characterisation of open foams using 3d images, Berichte des Fraunhofer ITWM, to appear